PHYSICAL REVIEW B VOLUME 26, NUMBER 12 15 DECEMBER 1982

Fast nonradiative recombination in sputtered *a*-Si:H

R. W. Collins,* P. Viktorovitch,† R. L. Weisfield, and William Paul
Gordon McKay Laboratory, Division of Applied Sciences, Harvard University, Cambridge, Massachusetts 02138
(Received 18 June 1982)

From measurements of the time decay of the relative luminescence efficiencies of samples of sputtered *a*-Si:H with different defect densities, we identify two low-temperature ($T \sim 80$ K) nonradiative recombination processes. In contrast with previously published analyses, we propose that the nonradiative recombination process most important in determining the steady-state luminescence efficiency at low temperature occurs for $t < 10$ ns and does not compete on the same time scale with the radiative transition.

I. INTRODUCTION

The decay of photoluminescence after termination of excitation has been studied in order to examine radiative and nonradiative processes in both glow-discharge and sputtered *a*-Si:H.[1–5] Tsang and Street[2,6] have measured the luminescence decay of several glow-discharge (gd) *a*-Si:H samples spanning a wide range of the low-temperature steady-state luminescence quantum efficiency. They have concluded that nonradiative recombination is the cause of an initial fast decay of luminescence observed on the scale of microseconds, since the magnitude of this decay was found to correlate inversely with the sample efficiency. The authors have interpreted these results in terms of nonradiative tunneling of band-tail electrons to randomly distributed, unoccupied defect states above the Fermi level. It is proposed that this process competes on the same time scale with the radiative transition. Searle *et al.*[7] and Nashashibi *et al.*[8] suggested a similar nonradiative tunneling mechanism to explain their decay results on both gd and sputtered *a*-Si:H and applied the formalism of the donor-acceptor pair model derived for crystalline semiconductors.

We have performed similar measurements on samples of sputtered *a*-Si:H, spanning nearly 3 orders of magnitude in low-temperature steady-state luminescence efficiency. By normalizing the data of the lower-efficiency samples to that of the highest-efficiency sample at each time of measurement, we eventually arrive at a simple alternative model of nonradiative recombination in sputtered *a*-Si:H. This model is consistent with measurements of the steady-state luminescence efficiency as a function of temperature and the correlation of the luminescence efficiency with the magnitude of the Fermi-level density of states.

II. EXPERIMENTAL

The samples of *a*-Si:H were prepared[9] by rf sputtering in Ar and H with the use of different H partial pressures (p_H) and/or substrate temperatures to obtain a variation in H content (c_H) from 7–30 at. %. The thicknesses of the samples are between 1 and 10 μm.

The measurements of the time dependence of the photoluminescence were carried out at 77 K with the use of 10-ns, 50-μJ pulses from a dye laser pumped by an N_2 laser. An $S1$ photomultiplier tube and boxcar integrator with a minimum gate width of 2 ns were used for detection and signal processing.

The detection energy was fixed at $\sim$0.25 eV above the peak position of the steady-state luminescence spectrum for each of the samples. Thus when we consider the time dependence of the luminescence intensity of one sample relative to another, the emission energy dependence of the time decay will be eliminated to first order. In addition, the excitation energy was fixed at $\sim$0.15 eV above E_{04} (the energy at which the absorption coefficient is 10^4 cm^{-1}) for each of the samples. Since the incident photon flux was maintained approximately constant for the samples, this ensures that the *absorbed* photon density was also approximately constant. To obtain the relative luminescence efficiencies in the time domain the data were corrected for the energy dependence of the sensitivity of the detection system.

The measurements of steady-state luminescence were carried out at 2.33-eV excitation energy and 10-mW intensity. The strong excitation intensity dependence of the shape of the luminescence intensity as a function of temperature due to nongeminate radiative recombination as reported by Street[10]

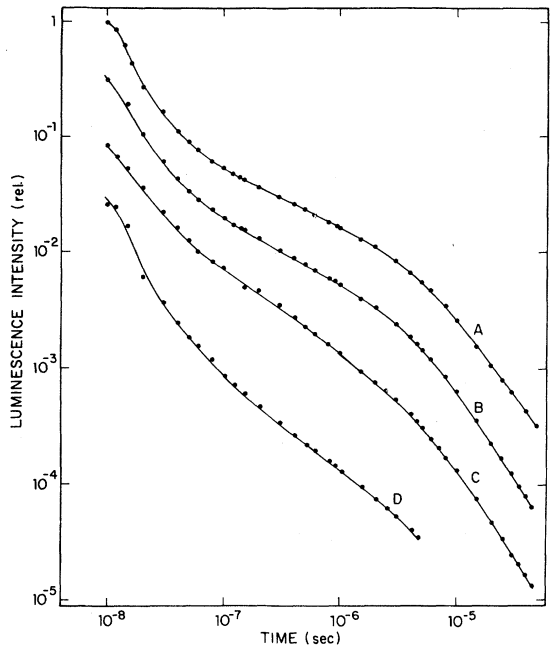

FIG. 1. Relative intensity of photoluminescence as a function of time for the four samples of Table I. The data were measured at emission energies 0.25 eV above the peak energies of the steady-state spectra for each of the samples.

was not observed[11] for our samples. The Schottky-diode admittance technique used to determine the Fermi-level density of states is discussed extensively elsewhere.[12]

III. RESULTS AND DISCUSSION

A. Time dependence

In Fig. 1 we show the relative intensity of photoluminescence as a function of time for four samples of sputtered a-Si:H, measured as described in Sec. II. The relative efficiences for the four samples at 10 ns and under steady-state illumination are given in Table I. The steady-state luminescence efficiency scales inversely with the defect density of the sample, and thus the samples in Table I span a wide range of defect densities (see Sec. III C). We obtain the curves in Fig. 2 by dividing the data for each of samples $B-D$ in Fig. 1 by the data of sample A at each time of measurement. Thus we obtain $I(N,t)/I(A,t)$, the luminescence intensity of sample N relative to that of sample A as a function of time. We propose that, due to the near unity-state luminescence efficiency of sample A, its luminescence time decay can be interpreted in terms of radiative recombination alone and that the deviation from this "ideal" behavior in samples $B-D$ can be attributed to nonradiative recombination due to the higher defect densities for these samples. As a result each of the curves in Fig. 2 can be interpreted as the nonradiative component to the decays of samples $B-D$ which can provide information on the processes that result in the sample-to-sample variations in the steady-state luminescence efficiency. The results show that the order-of-magnitude variations in the luminescence efficiency with sample cannot be attributed to nonradiative processes that occur after 10 ns which lead to the relative efficiencies in the final column of Table I. Instead, the sample-to-sample variations in steady-state efficiency are due primarily to recombination that occurs before 10 ns [see I(10 ns) in Table I]. Changes in the relative efficiency as a function of time (for $t>10$ ns) occur only for $t>200$ ns in sample B, $t>100$ ns in sample C, and $t>20$ ns in sample D. These changes are most dramatic for the lowest-efficiency samples and weaken as the sample efficiency increases. In the following discussion we will develop a simple model of nonradiative recombination in a-Si:H to explain these results.

For the purposes of our discussion we will assume that the hole is immobile during thermalization and relaxation and that the photoluminescence is quenched when the electron escapes from the hole. This may be the case if the thermalization and relaxation of the hole proceed on a time scale faster than that of the electron. Faster hole thermalization and relaxation would be expected if the hole is more strongly coupled to the lattice; alternatively, faster hole relaxation would occur if the

TABLE I. Relative photoluminescence efficiencies in the time domain for sputtered a-Si:H.

Sample	p_H (mTorr)	c_H (at. %)	I(steady state) (rel.)	I(10 ns) (rel.)	I(steady state)/I(10 ns)
A	2	30	1	1	1
B	1.6	16	0.3	0.4	0.8
C	0.4	8	0.04	0.1	0.4
D	0.1	7	0.006	0.03	0.2

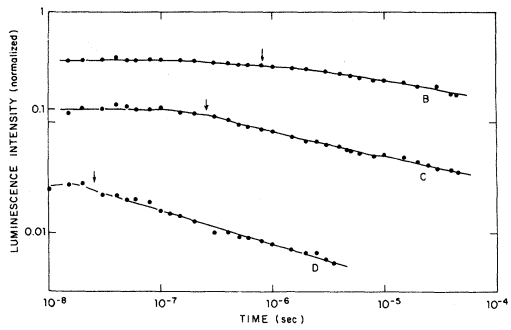

FIG. 2. Data of Fig. 1 for samples $B-D$, normalized to the data for sample A.

rigid-band density-of-states tail above the valence-band edge were more extensive than that below the conduction-band edge.

We will also make a note on the semantics of our discussion. In order to deplete the electron population available for radiative recombination, it is only necessary for the electron to escape completely from the hole. The actual nonradiative recombination may or may not occur at this time. In the following, we use the terms "nonradiative process" and "nonradiative recombination" to denote any event by which an electron escapes from the hole, thus losing all chance of subsequent radiative recombination. With the above clarifications presented we will proceed to describe our model in detail.

We first propose that the fast nonradiative recombination ($t<10$ ns) occurs during thermalization or before deep trapping when the photoexcited electrons are still relatively mobile. Any electron excited within one thermalization radius[13] $R_{\rm th}$ of a nonradiative recombination center may be captured and recombine very rapidly ($t<10$ ns). The surviving electrons relax more deeply into localized states and can recombine nonradiatively at low temperature only by tunneling. Thus in a sample of sufficiently low density of nonradiative recombination centers such that the average distance between the centers, $R_{\rm nr}$, satisfies $R_{\rm nr}\gg R_{\rm th}$, most further nonradiative recombination will be expected to occur on a much later time scale. This may explain the constant relative efficiency for $10<t<200$ ns in sample B. As the density of nonradiative centers increases, however, the surviving electrons undergo nonradiative tunneling at shorter times in accordance with the relation[6]

$$t=\tau_0\exp(2R/R_0)\,, \tag{1}$$

where t is the time necessary for the tunneling event, R is the distance from the electron to the nonradiative center, R_0^{-1} is the localization parameter of the electron, and τ_0^{-1} is an attempt frequency. This appears to explain the shift of the apparent onset of the slow decay observed in Fig. 2 to shorter times for samples of higher defect density (as deduced from the relative steady-state efficiency values; see Sec. III C). The arrows in Fig. 2 identify the times at which the luminescence intensities have decreased 10% relative to the values obtained at 10 ns.

B. Temperature dependence

Thus our interpretation suggests that although a nonradiative process attributed to tunneling (which competes on the same time scale as the luminescence) can be identified, the primary mechanism of nonradiative recombination at low temperatures occurs at times much shorter than those of the radiative transition process. Additional evidence in support of this conclusion comes from measurements of the temperature dependence of the steady-state luminescence intensity $I(T)$. The general form for $I(T)$ when luminescence is geminate is[14]

$$I(T)\propto Y_0\left[\frac{p_{\rm r}}{p_{\rm nr}^{\rm act}+p_{\rm nr}^{\rm tun}+p_{\rm r}}\right]. \tag{2}$$

In this expression $p_{\rm r}$ is the probability of radiative recombination, $p_{\rm nr}^{\rm act}$ is the probability of nonradiative recombination via thermal activation of the electron to the conduction band resulting in capture by an unoccupied defect state, and $p_{\rm nr}^{\rm tun}$ is the probability of nonradiative tunneling of the electron directly into a defect state (see Fig. 3). Y_0 represents a noncompetitive process such as the direct capture of thermalizing carriers by nonradiative recombination centers proposed above. In general $p_{\rm nr}^{\rm act}$ will depend on the conduction-band tail-state distribution as described elsewhere,[15] whereas $p_{\rm nr}^{\rm tun}$ and Y_0 will depend on the density of nonradia-

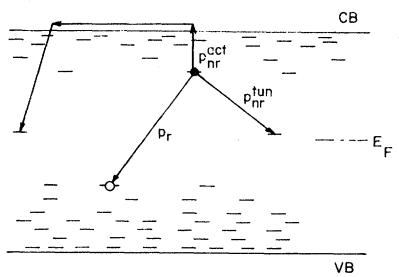

FIG. 3. Two possible processes resulting in nonradiative recombination at high temperature on the same time scale as the luminescence transition.

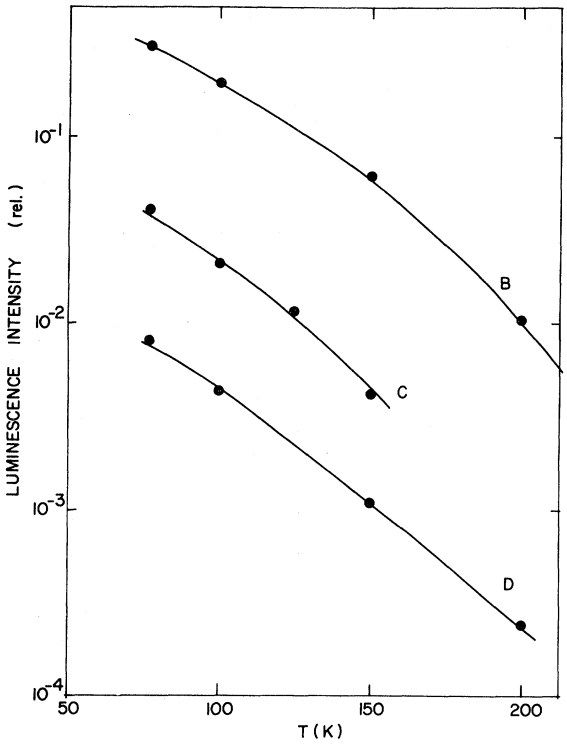

FIG. 4. Peak steady-state luminescence intensity as a function of temperature for samples $B-D$.

tive recombination centers. In Fig. 4 we show $I(T)$ for samples $B-D$ of Table I. The spectral widths of the luminescence for the three samples are the same within 5% and suggest that the tail-state distributions, and thus $p_{\rm nr}^{\rm act}$, do not show significant sample dependences. The parallel nature of the three curves suggests that $p_{\rm nr}^{\rm tun}$ is not an important contribution to the denominator of Eq. (2) and that Y_0, the noncompetitive factor, is the primary factor that determines the low-temperature efficiency of these samples. If the reverse were the case, we could easily make measurements at a temperature where $p_{\rm nr}^{\rm act} \gg p_{\rm nr}^{\rm tun}$ and, for all samples, independent of the density of nonradiative recombination centers, $I(T)$ would approach the same value. Thus from the temperature dependence of the steady-state luminescence magnitudes for these samples, we also conclude that the low-temperature luminescence efficiency in sputtered a-Si:H is determined for the most part by nonradiative recombination that does not compete on the same time scale with the luminescence.

C. Correlation with the Fermi-level state density

Next we shall use these results to develop a simple model to explain the observed relationship between the low-temperature luminescence efficiency and the magnitude of the Fermi-level density of states N_F. Earlier work has suggested that although a-Si:H sputtered at low $p_{\rm H}$ has a high density of nonradiative recombination centers, it does not have a band tail-state distribution significantly different from that of samples of high luminescence efficiency.[15] We thus associate these centers with states at midgap measureable by our density of states technique.

We neglect the nonradiative process due to competitive tunneling and suppose that after excitation a thermalizing electron can either be trapped by a localized state in the conduction-band tail, leading to radiative recombination, or it can be captured by a midgap state in a radiationless transition. Thus the low-temperature luminescence efficiency ($p_{\rm nr}^{\rm act} \ll p_{\rm r}$) can be expressed as follows:

$$Y_0 = \frac{\beta_t N_t}{\beta_t N_t + \beta_{\rm nr} N_{\rm nr}} , \tag{3}$$

where N_t and $N_{\rm nr}$ are the spatial densities of tail states and nonradiative centers, respectively. The quantities β_t and β_{nr} are average capture cross sections for the two types of states. We suggest that $\beta_{\rm nr}/\beta_t N_t$ is sample independent[16] and that we can replace $N_{\rm nr}$ by $N_F \Delta E$, where ΔE is the energy extent of the distribution of nonradiative centers.

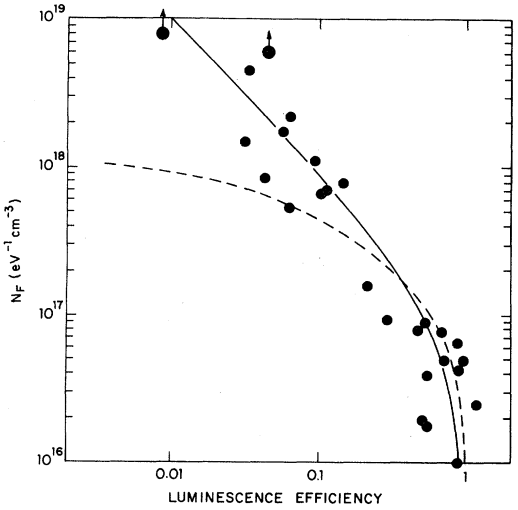

FIG. 5. Correlation between the steady-state luminescence efficiency Y_0 measured at 77 K, and the Fermi-level density-of-states magnitude for several samples of sputtered a-Si:H. The arrowed data points denote samples with weak photoluminescence for which only a lower limit of N_F could be deduced from the admittance technique. The solid line shows the result predicted from Eq. (4) with $A = 1 \times 10^{-17}$ cm^{3}eV. The dashed line represents the results predicted from the model in Ref. 2.

Equation (3) becomes

$$Y_0=(1+AN_F)^{-1}\,, \tag{4}$$

where $A=\beta_{nr}\Delta E/\beta_t N_t$. We include in Fig. 5 the result predicted from Eq. (4) using a value of $A=1\times10^{-17}$ cm^{3}eV, chosen to give a reasonable fit to the experimental data (see solid line). The broken line in Fig. 5 represents a best fit of the data to the predicted result of Tsang and Street, based on a model of competitive tunneling to a random distribution of nonradiative recombination centers.[17] The closer fit of Eq. (4) to our experimental results suggests that, at least for sputtered samples, the model of fast nonradiative recombination we have proposed may be more appropriate.

From the value of A in Eq. (4), using $\Delta E=1$ eV,[18] we can find β_{nr}/β_t for a reasonable estimate of the total density of tail states. Figure 6 shows β_{nr}/β_t as a function of N_t, with $\Delta E=1$ eV. For a reasonable value of $N_t=10^{19}$ cm^{-3}, from Fig. 6, we find that $\beta_{nr}/\beta_t=10^2$, suggesting a much higher capture cross section for the nonradiative centers. While any statement about the nature of the nonradiative centers must be rather speculative, it seems plausible that the difference between the tail states and the nonradiative recombination centers in the gap is that the former are uncharged when empty whereas the latter are charged. This proposal is consistent with the observation of a relatively high capture cross section for electrons by deep levels near midgap from admittance measurements performed on our samples.[12] Our results are not inconsistent with the suggestion that nonradiative recombination occurs through unoccupied dangling-bond states.

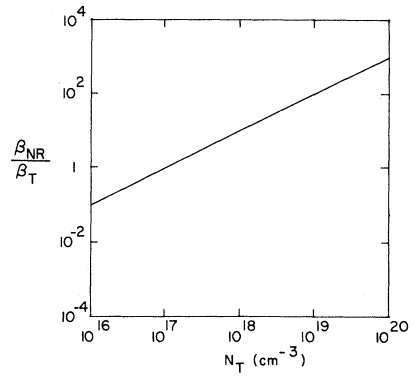

FIG. 6. Ratio of the average capture cross section for nonradiative centers to that of tail states vs the total density of tail states. This relationship has been determined from the value of A found to fit the data of Fig. 5, with ΔE, the energy extent of the distribution of nonradiative recombination centers, arbitrarily taken equal to 1 eV.

IV. CONCLUSION

From the relative luminescence efficiencies as a function of time for several samples of sputtered *a*-Si:H we conclude that two low-temperature ($T\sim80$ K) nonradiative recombination processes can be identified. One process occurs for $t<10$ ns and does not compete on the same time scale with the radiative transition. It is proposed that this fast recombination occurs via the capture of either thermalizing or weakly localized electrons by nonradiative recombination centers near midgap and is most important in determining the sample-to-sample variations in the steady-state luminescence efficiency. The second process sets in at a later time and is associated with the competitive tunneling of more strongly localized electrons to the nonradiative recombination centers. This model is consistent not only with the time-dependent luminescence measurements but also with measurements of the temperature dependence of the steady-state luminescence efficiency and with the correlation between the low-temperature luminescence efficiency and the midgap state density.

ACKNOWLEDGMENTS

We thank Suha Oguz for measurements of the hydrogen content and James Eggert, Paul Kirby, Djalil Lachter, Suha Oguz, Bolko von Roedern, and Ben Yacobi for a critical reading of the manuscript. We also acknowledge P. Ketchian for assistance in sample preparation. Funding was provided by the NSF under Grants Nos. NSF-DMR78-10014 and NSF-DMR81-08327.

*Present address: Standard Oil Company (Ohio), Broadway Laboratory, 3092 Broadway Avenue, Cleveland, OH 44115.

†Present address: Ecole Centrale de Lyon, European Research Associates, Centre National de la Recherche Scientifique, Genie Electronique (no. 661), 36 Route de Dardilly, F-69130 Ecully, France.

[1]D. Engemann and R. Fischer, in *Structure and Excitations of Amorphous Solids, Williamsburg, Va., 1976,* Proceedings of an International Conference on Struc-

ture and Excitation of Amorphous Solids, edited by B. Lucovsky and F. Galeener (AIP, New York, 1976), p. 37.

[2]C. Tsang and R. A. Street, Philos. Mag. B 37, 601 (1978).

[3]I. G. Austin, T. S. Nashashibi, T. M. Searle, P. G. LeComber, and W. E. Spear, J. Non-Cryst. Solids 32, 373 (1979).

[4]S. Kurita, W. Czaja, and S. Kinmond, Solid State Commun. 32, 879 (1979).

[5]W. Rehm and R. Fischer, Phys. Status Solidi 94, 595 (1979).

[6]C. Tsang and R. A. Street, Phys. Rev. B 19, 3027 (1979).

[7]T. M. Searle, T. S. Nashashibi, I. G. Austin, R. Devonshire, and G. Lockwood, Philos. Mag. B 39, 389 (1979).

[8]T. S. Nashashibi, T. M. Searle, I. G. Austin, K. Richards, M. J. Thompson, and T. Allison, J. Non-Cryst. Solids 35-36, 675 (1980).

[9]D. A. Anderson, G. Moddel, M. A. Paesler, and W. Paul, J. Vac. Sci. Technol. 16, 906 (1979). See also W. Paul and D. A. Anderson, Sol. Energy Mater. 5, 229 (1981).

[10]R. A. Street, Phys. Rev. B 23, 861 (1981).

[11]R. W. Collins and W. Paul, Phys. Rev. B 25, 5263 (1982).

[12]P. Viktorovitch and G. Moddel, J. Appl. Phys. 51, 4847 (1980).

[13]See, for example, E. A. Davis, J. Non-Cryst. Solids 4, 107 (1970).

[14]See, for example, R. A. Street, Adv. Phys. 25, 397 (1976).

[15]R. W. Collins and W. Paul, Phys. Rev. B 25, 5257 (1982).

[16]This is true for our sputtered samples, but probably also for all *a*-Si:H, howsoever prepared, which exhibit comparable band tails as evidenced by the spectral width of the luminescence and the temperature dependence of the luminescence efficiency (Ref. 15).

[17]The curve shown uses the relationship from Ref. 2, $Y_0=\exp[(4\pi R_c^3 N)/3]$, where R_c is a critical tunneling distance between the electron and the nonradiative recombination center and N is the density of nonradiative recombination centers. We assume that $N \sim N_F \Delta E$ and take $R_c^3 \Delta E = 1.2 \times 10^{-18}$ cm^3 eV.

[18]The choice of $\Delta E = 1$ eV is arbitrary. If we were to speculate that dangling bonds provide the nonradiative centers, then ΔE would be less than a correlation energy. Thus it would be likely that $\Delta E < 1$ eV. This would make our argument associated with Fig. 6 even stronger.